RSC Advances

ROYAL SOCIETY OF CHEMISTRY

www.rsc.org/advances

RSC Advances

PAPER

Mechanism of oil molecules transportation in nano-sized shale channel: MD simulation

Qingzhong Xue,[ab]***** **Yehan Tao,**[ab] **Zilong Liu,**[a] **Shuangfang Lu,**[c]***** **Xiaofang Li,**[a] **Tiantian Wu,**[a] **Yakang Jin,**[a] **Xuefeng Liu**[b]

Unconventional energy such as shale oil & gas opens up a new avenue for alleviating the pressure of conventional energy crisis, enabling the sustainable development of economy and industry. We firstly explored the mechanism of oil molecules transportation in nano-sized shale channel by molecular
10 dynamic simulations. It is demonstrated that the competition between the oil adsorption strength to shale surface and the driving force from gas flooding (N_2) plays the dominant role in oil translocation process in shale channel. The encapsulated oil molecules would be expelled by gas flooding when the gas pressure reaches a critical value. Besides, it is found that the pressure of the gas flooding, shale channel pore size, N_2 amount, temperature and shale components all have important effect on the translocation
15 process of oil molecules inside shale channel, whose oil-driving efficiency is characterized by oil displacement distance and oil displacement loss. This work lays a theoretical foundation to achieve effectively and efficiently exploiting oil. Besides, the result may shed light on explaining many industrial processes and natural phenomena in nano-sized channels, including viscous liquid transport or diffusion through membrane, energy conversion devices, biological molecules (hemoglobin, protein, DNA)
20 translocation and so forth.

Introduction

The rapid development of economy and society witnesses an increasing requirement for energy, but unfortunately, due to the excessive consumption of conventional energy, the contradiction
25 between the supply and demand of energy becomes more prominent, posing a challenge to the sustainable development of human society. Unconventional oil has triggered off enormous scientific interest due to its huge reserves,[1,2] which endows it with great potential to release the stress of conventional energy
30 crisis.[3,4,5] Shale oil is short for mature-organic shale oil, the most representative energy listed under the unconventional energy headings, which refers to the petroleum preserved in those nano-scale pores in organic-rich shale.[6] In order to pave the way for further exploration, including optimizing production and
35 determining economic feasibility, knowledge of physical aspects of shale oil storage and transport mechanism is urgently required. A lot of effort has been made to explore the interface interaction between oil or gas/substrate,[7,8,9] oil/oil-displacing agent,[10] oil-

[a]State Key Laboratory of Heavy Oil Processing, China University of
40 *Petroleum, Qingdao 266580, Shandong, P. R. China*
[b]College of Science, China University of Petroleum, Qingdao 266580, Shandong, P. R. China
[c]Institute of Unconventional Oil & Gas and New Energy, China University of Petroleum, Qingdao 266555, Shandong, P. R. China
45 *E-mail:* xueqingzhong@tsinghua.org.cn; Tel: 86-0532-86981169; Fax: 86-0532-86981169; lushuangfang@qq.com

displacing agent/substrate,[11,12,13] or ternary phase interaction.[14,15,16] Besides, the formation mechanism of shale oil is widely
50 investigated.[6,17,18] Although much progress has been achieved in both theoretical and experimental studies on shale oil storage, the most important question of how oil molecules transport in shale channels remains unanswered.

Shale oil, generally light oil with low viscosity, occurs in
55 adsorption state in nanoscale shale channels, which is a common consequence of the attractive interaction between adjacent oil molecules and the attractive interaction between oil molecules and channel walls. This renders oil molecules really difficult to transport in shale channels without the assistance of an external
60 driving force. Water flooding and gas flooding are common external driving force in bulk systems. However, since oil recovery from water flooding relies on the spontaneous imbibition of water to expel oil from the matrix into the fracture system. In oil- or mixed-wet shale reservoirs, the capillary
65 driving force for the spontaneous imbibition process is weak, and therefore the water flooding oil recovery efficiency is low.[15] Gas flooding is not restricted by the wettability of shale surface because the interaction between gas molecules and shale reservoirs is much weaker. Therefore, the gas flooding may be an
70 effective method to exploit shale oil.

Diameter of pores in shale oil sediments ranges from only a few nanometers to a few micrometers, which means the transport process of shale oil in shale system is different from that in bulk
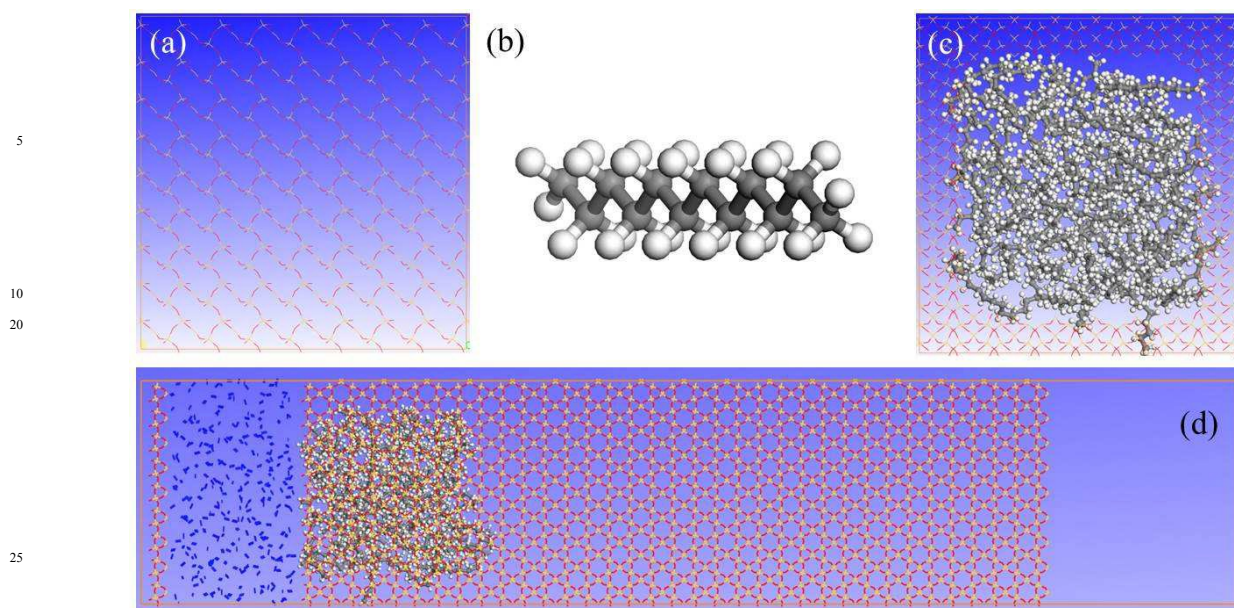
Fig. 1 (a) Silica surface, (b) dedecane molecule, (c) 3 nm silica channel with 74 oil molecules inside, (d) N_2 driving oil transport model.

system due to the high surface-to-volume ratio in shale channels. This makes the evaluation of the gas driving oil transport process inside shale channels using conventional laboratory techniques to be a challenging problem. In addition, because of the size restriction, Cauchy and Navier-Stokes equations, which can be used to derive the Poiseuille and other continuum-level flow relations, cannot be applied in nano-sized fluid, thus hindering our further understanding of the mechanism of oil transportation in nano-sized channels. The molecular scale boundary characteristics, which are determined by the fluid-solid interaction, are important in understanding the behavior of oil flow in shale channels. Recently, it has been demonstrated that molecular dynamics (MD) simulation is a powerful method to understand the transport mechanism in nano-sized systems.[19,20,21,22,23] For instance, MD simulation has been widely used to study the nanofluid, such as water flow inside carbon nanotubes,[20,21,24,25,26,27] argon transport inside a nanopore[19] and surfactant filling carbon nanotubes.[22] Furthermore, Yu et al employed MD simulation to study the transport of water molecules along carbon nanotubes under the driving force of methane molecules.[28] Our group has investigated the release of encapsulated molecules from carbon nanotubes using a displacing method by MD simulation.[29]

In this paper, the mechanism of oil molecules transported in nano-sized shale channel was intensively studied using MD simulations. It is found that the pressure of filling gas, shale pore size, N_2 amount, temperature and shale components should all be taken into consideration in the translocation process of oil molecules inside nano-sized channel. The MD simulation provides further information for the fundamental understanding of oil translocation process in nanoscale channels, which is conducive in guiding the oil-displacing gas design, oil recovery enhancement, ore flotation, detergency and printing. Moreover, our investigations hold sway on many biological applications including DNA and RNA transport through cell membrane, gene swapping between the guest and host bacteria through pili, etc. as

well as many other fields such as membrane separation of mixtures, gas storage device, electro kinetic micron size channel battery and so on.[19,30,31,32,33,34]

Modeling and methods

MD simulation method was employed to simulate the infinite system. The interatomic interactions were described by the force field of a condensed-phase optimized molecular potential for atomistic simulation studies (COMPASS).[35] COMPASS is a parameterized, tested and validated first *ab initio* force field, which enabled accurate and simultaneous prediction of various gas-phase properties and condensed-phase properties of most of common organic and inorganic materials.[36,37,38] The Anderson thermostat method was employed to control the temperature of the system, the VDW interactions were calculated within a cutoff distance of 9.5 Å, and the Ewald method was applied for the calculation of electrostatic interactions.[38,39,40,41,42] Interactions between oil molecules, gas molecules, oil molecules and gas molecules, oil or gas molecule and shale channels, were treated using a Lennard - Jones potential, which has been widely used to describe the above interactions in shale system.[7,8,9,10,12,14] Periodic boundary conditions were applied in all three dimensions.

In our work, silica (Fig. 1(a)) and dodecane ($C_{12}H_{26}$) (Fig. 1(b)) are selected as the typical component of the shale substrate and oil droplet, respectively. The shale channel model was constructed by building a silica supercell with dimensions of 44.217Å × 43.242Å × 148.917Å and digging a 3 nm square hole in the middle of the supercell along the direction of z axis (as seen in Fig. 1(c)). A vacuum of 38 Å was constructed along the direction of z axis to eliminate the effect of periodic boundary condition. Then 74 dodecane molecules were inserted into the hollow cavities of the silica supercell near the left end of the channel. To find the thermally stable morphology of oil molecules inside a shale channel and achieve a configuration with minimum potential energy, energy minimization was performed. Due to the mixed-wet silica surface, arousing an attractive force
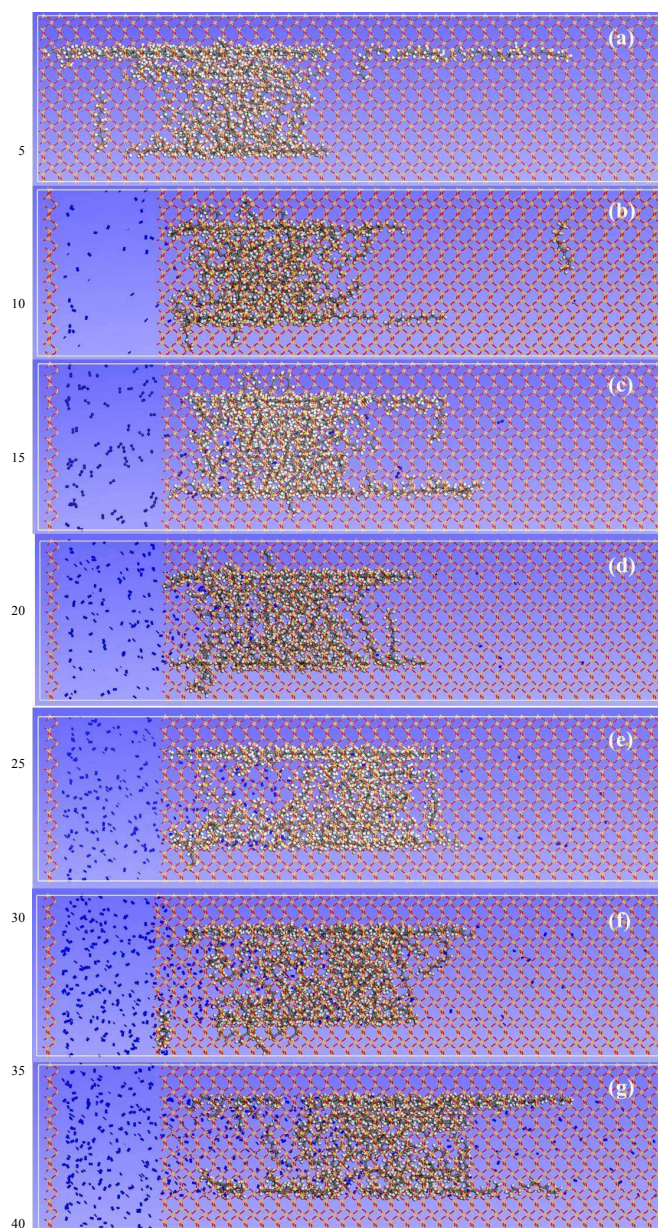
Fig. 2 Final configurations of oil molecules inside silica shale channel after N₂ driving - with N₂ initial pressure of (a) 0 Mpa, (b) 5 Mpa, (c) 10 Mpa, (d) 20 Mpa, (e) 30 Mpa, (f) 40 Mpa and (g) 50 Mpa. Red, yellow, grey, white and blue balls represent O, Si, C, H and N atoms, respectively.

45 for oil molecules, the oil droplet was intensively adsorbed inside the channel and almost kept its initial shape.[14] This minimum energy conformation was used as the initial status in the following MD simulations. The gas flooding, namely, N₂ molecules flooding, was initially placed near the opening at left 50 end of the shale channel along the direction of z axis. Six types of N₂ boxes with same box parameter but different gas initial pressures were set up to study the "start-up pressure" for N₂ driving oil transport in shale channel. A thin silica wall was put at the other side of N₂ box to prevent the diffusion of N₂ molecules 55 directly into the vacuum phase because of the periodic boundary condition. The silica channel and wall were kept fixed. The total length of the model was 217.65 Å (see in Fig. 1(d)).

We then put the model into a NVT ensemble, a fixed time step of 1 fs was used and data was collected every 5 ps. A 2.5 ns 60 simulation time was performed for all calculations. The full-precision trajectory was then recorded, and the results were analyzed. Our MD simulations were carried out using Discover code embedded in the Material Studio software.

Results and discussion

Start-up pressure

The strength of driving force has great influence on the transport process of oil molecules inside nano-sized silica shale channel, thus we first determine the candidate start-up pressure for N₂ flooding. Shale oil generally occurs in adsorption state in 70 nanoscale shale channels, which is a common consequence of the attractive interaction between adjacent oil molecules and the attractive interaction between oil molecules and channel walls. The applied external force need to overcome this attractive interaction to realize the translocation process of oil droplet. As 75 we can see in Fig. 4 (a) and (b), the translocation distance less than 15 Å (the radius of oil droplet) is not obvious, which has no meaning for the industrial exploiting of shale oil. So we consider that only the external pressure make oil droplet have a translocation distance more than 15 Å, and this external pressure 80 can be called the "start-up" pressure. Six types of N₂ pressures were simulated, with initial pressure intensity of 5 Mpa, 10 Mpa, 20 Mpa, 30 Mpa, 40 Mpa and 50 Mpa, respectively, and for comparison, a shale oil model without N₂ flooding (0 Mpa) was also constructed (see in Fig. 2(a)). Then, we performed a 2.5 ns 85 dynamic process to observe the oil translocation process. Furthermore, the oil concentration profiles along z axis were calculated, the left end of the model was set as zero point, as shown in Fig. 3. For clarity, we just show the oil concentration profiles of 0 Mpa, 5 Mpa, 30 Mpa and 50 Mpa, while other oil 90 concentration profiles for 10 Mpa, 20 Mpa and 40 Mpa can be found in Figure s1 of Supporting Information. The peak in the curve of oil concentration profile is defined as the center of oil droplet and the difference between the oil centers in the silica
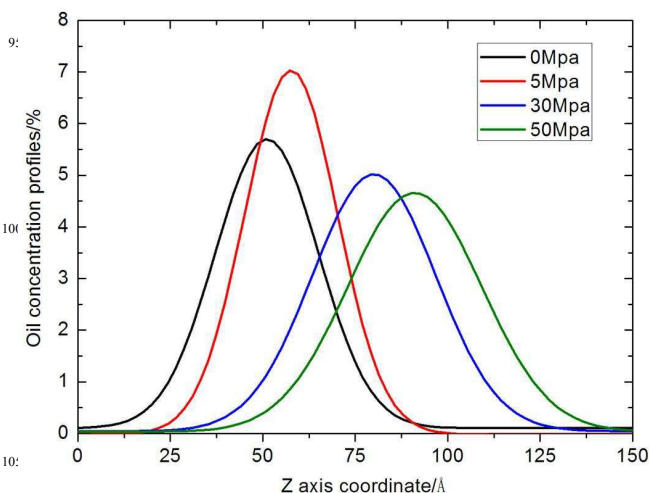

Fig. 3 Oil concentration profiles (Gaussian fitting) in final configuration of N₂ driving oil transport inside silica shale channel with N₂ initial pressure of 0 Mpa, 5 Mpa, 30 Mpa and 50 Mpa.

shale channel under 0 Mpa and that under other N$_2$ pressure is regarded as the oil displacement distance under N$_2$ driving. Combined Fig. 2 and Fig. 3, during a 2.5 ns simulation, no obvious oil translocation is observed under 0 Mpa model, except for a small amount of oil molecules spreading on silica surface because of the vdW interaction between oil molecules and silica surface. This illustrates that dodecane molecules prefer to stay near the surface of silica and cannot transport in silica shale channels spontaneously without the help of a driving force.
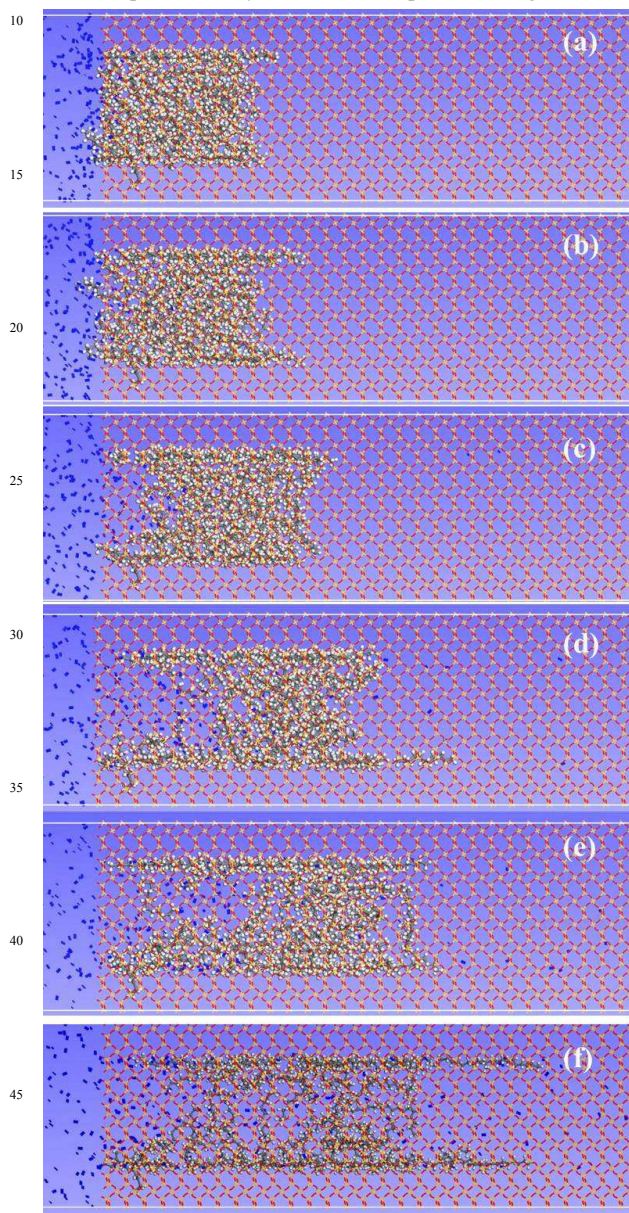

Fig. 4 Snapshops of the oil molecules transport process in silica shale channel at (a) 0 ps, (b) 250 ps, (c) 1000 ps, (d) 2000 ps, (e) 2500 ps and (f) 3500 ps.

Compared to that without injecting N$_2$ flooding, oil droplets with a driving force of 5-20 Mpa reveal a very small displacement distance (less than 12 Å), which means the driving force coming from these low-pressure N$_2$ flooding is not sufficient to give rise to the transport of oil molecules. An apparent translocation is shown in 30 Mpa model, where the oil

center has a displacement of about 26.827 Å. When the N$_2$ pressure further increased to 40 Mpa, the displacement are similar to that of 30 Mpa. But there is another obvious growth of oil displacement in 50 Mpa model, with an oil displacement distance of approximately 33.48 Å. The displacement distance witnesses an increase with the ascending N$_2$ pressure, but notice that 30 Mpa has the optimal balance between the oil recovery and economic feasibility among the pressures we tested because higher N$_2$ pressure means higher operation difficulties and the risk of gas storage and transport increased, so we performed all the following discussions based on 30 Mpa model. Of course the start-up pressure is decided by many factors as we discussed below, such as the oil and shale component, the pore size of the channel, temperature and so forth. Therefore, we are only able to give the relation between two factors. For example, the relation between the pore size and the applied nitrogen pressure can be calculated by fixing the pore size and changing the applied nitrogen pressure. So 30 Mpa is only the cutoff pressure for 3 nm oil droplet inside 3-5 nm silica channels at 298 K.

Transport process

The transport process of oil molecules inside nano-sized silica shale channel under 30 Mpa is shown in Fig. 4. And, the whole dynamic process can be seen in Video S1 of Supporting Information. The initial optimized configuration is shown in Fig. 4(a). Because of the presence of N$_2$ flooding, the oil molecules begin to transport in the silica shale channel. The whole process can be divided into three stages. In the first stage, before 500 ps, N$_2$ flooding can be seen as compressed N$_2$ which can generate a driving force and induce the transport of oil droplet inside the silica shale channel. Theoretically, dodecane molecules become unstable thermodynamically and the aggregates of oil molecules are disturbed. Simultaneously, the structural change of oil droplet is observed, as seen Fig. 4(b) at 250 ps.

The second stage corresponds to the oil droplet translocation process before 1000 ps. With the N$_2$ molecules filling into the channel and occupying the cavity space, the oil molecules are gradually expelled from the channel. The oil molecules near the N$_2$ flooding move forward and the adjacent oil molecules continuously moved to the right side of the channel, due to the interaction among oil molecules. The former oil molecules on the right side of the oil droplet near the silica surface become adsorbed during the movement because of the attractive interaction of the silica surface and its cavity would be replaced by the back oil molecules.

Finally, the translocation of oil molecules inside the channel occurred after 1000 ps simulation and the oil molecules start to move to the other side of the channel under the driving of N$_2$ molecules. It should be noticed that the oil molecules adsorbed on silica surface remains difficult to be expelled by N$_2$ flooding, the main reason is that the strong adsorption energy of silica surface acts as an energy barrier preventing oil molecules near silica surface from running away, thus forming an adsorption layer on the surface of silica, the thickness of which is about one oil molecule size. As the increasing of the adsorbed layer, the diameter of the oil droplet becomes smaller during the translocation process and undeniably causes the loss of oil during the exploiting process. Another point should be pointed out is that

in the whole process, N_2 molecules demonstrate poor dissolution ability into the oil molecules because few N_2 molecules are observed to diffuse into the oil droplet, which is beneficial to the driving of oil molecules. The pressure of N_2 decreases to some extent because of the diffusion of N_2 molecules in the channel.

Pore size effect

In nanoscale, the effects of volume forces which dominate the fluid properties in the large scale are weakened, and the impacts of surface forces are enhanced. A key topic in the studies of flow in nanochannel is how the interaction between the fluid molecules and the surface will affect the liquid flow. In general, this interaction depends greatly on surface-to-volume ratio of the channel, which is very big in shale channels. This is because the pore diameter of shale channel is only a few nanometers and the smaller the pore size is, the bigger the surface-to-volume ratio is. To further study the effect of surface-to-volume ratio on the transport of oil molecules, we study the transport of oil molecules through other two kinds of silica shale channels with different pore sizes. The pores of the silica shale channels considered are 4
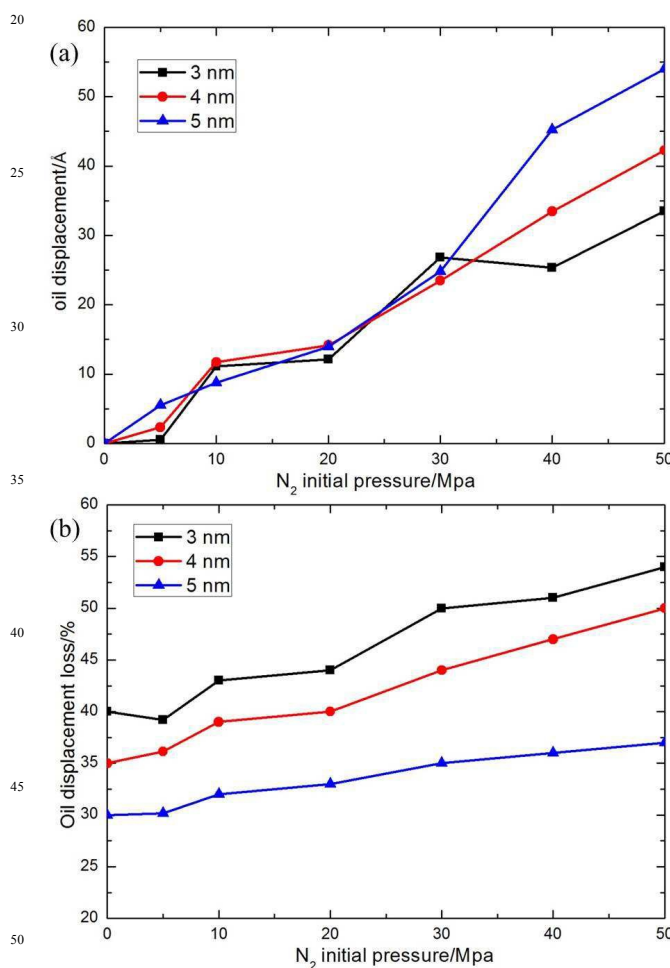

nm and 5 nm square pores in the middle of the silica supercell. Six types of N_2 pressures were simulated, with same initial pressure intensities as that of 3 nm model. The oil displacement inside different pore size silica shale channels under different N_2 initial pressure are shown in Fig. 5(a).

During a 2.5 ns simulation, little oil translocation is observed for 0 Mpa model, in spite of the spread of a small amount of oil molecules on silica surface because of the attractive interaction between the oil molecules and silica surface. For all three kinds of channels, before adding a N_2 flooding of 30 Mpa, the oil displacements are not obvious (less than 15 Å) and demonstrate a slow climbing tendency with the growing of the N_2 driving pressure and the displacement distance is quite similar for three kinds of pore size. Whereas, a rather different case is observed when a 30 Mpa N_2 initial pressure is applied. The oil displacement distance witnesses a significant rise to about 30 Å, almost double that under 20 Mpa. The oil displacements of 3 nm pore at 30 Mpa and 40 Mpa are similar and this difference can be ignored in our system. In fact, the oil displacement of 3 nm pore is smaller than that of 4 nm and 5 nm pore under 40 Mpa and 50 Mpa because of the stronger average attractive interaction between oil molecules and silica channel, which means it is really hard to stimulate the translocation process in small shale channels. The differences of oil displacements are obvious at higher applied pressure. When we further increase N_2 initial pressure, the oil displacement distance in different pores varies differently from each other. The oil displacement in the 3 nm channel with the smallest pore size displays the smallest oil displacement distance and does not see any further increase under higher N_2 initial pressure. However, the oil displacement in the 4 nm and 5 nm channels displays an apparent increase under higher N_2 initial pressure and the biggest (5 nm) channel shows the biggest oil displacement distance.

In addition to the oil displacement distance, we found that the oil displacement loss varies greatly with pore size. The oil displacement loss is defined as the ratio between the number of oil molecules "adsorbed" on the silica surface and the number of total oil molecules in our simulation. It should be pointed out that if over half of the atoms in a single molecule are adsorbed on the silica surface, we consider that this molecule is "adsorbed". The

Fig. 5 (a) Oil displacements inside different pore size silica shale channels under N_2 pressure from 0 ~ 50 Mpa. (b) Oil displacement loss inside different pore size silica shale channels under N_2 pressure from 0 ~ 50 Mpa.
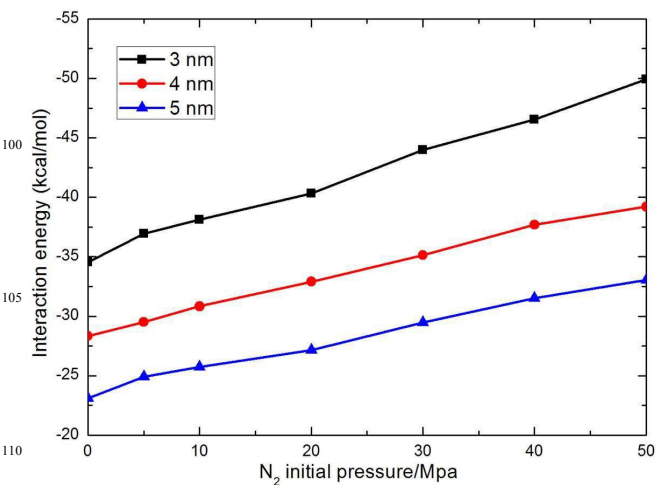

Fig. 6 Average adsorption strength of oil molecules to different shale channels under N_2 pressure from 0 ~ 50 Mpa.

oil displacement loss of three different pore size models under different N_2 initial pressure are shown in Fig. 5(b). The oil displacement loss witnesses an increasing trend as the decreasing of the pore size, which means that oil molecules in the smaller pore channel prefer to stay on surface of the silica surface rather than moving under the driving of the N_2 flooding. It is the competition between the average adsorption strength of oil molecules to silica surface and the driving force from the gas flooding plays a significant role on the oil displacement loss. In smaller pore channel, the average adsorption strength of oil molecules to silica surface occupies the dominant status and oil molecules are strongly adsorbed on the silica surface, causing the oil displacement loss in the driving process. Whereas, the driving force coming from the N_2 flooding reveals its advantage in larger pore channel, in which the average adsorption strength of oil molecules to silica surface is greatly weakened, thus the smaller oil displacement loss is expected.

From the above discussions, it is identified that the average adsorption strength of oil molecules to the shale surface has a great influence on the oil transport process. We calculate the interaction energy between oil molecules and shale channels to evaluate the average adsorption strength of oil molecules, and it could be calculated as follows:

$$E_{oil/silica} = \frac{(E_{oil} + E_{silica}) - E_{total}}{N_{oil}} \qquad (1)$$

where $E_{oil/silica}$ is the interaction energy, N_{oil} is the number of the oil molecules, E_{oil} and E_{silica} refer to the energy of oil components
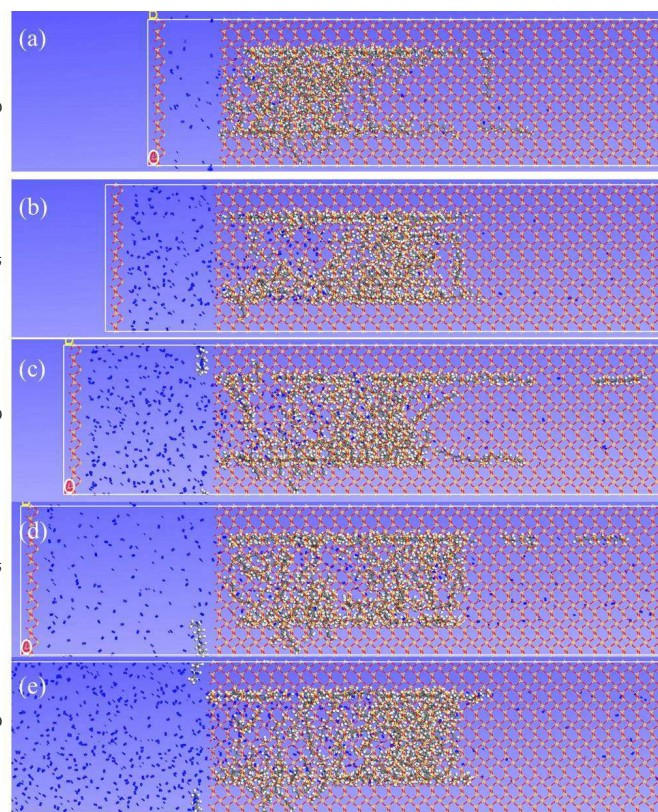
and silica surface, respectively, E_{total} represents the total energy of oil and silica surface. These calculated average adsorption strength of oil molecules as a function of N_2 initial pressure are shown in Fig. 6. It can be found that the trend of interaction energy increased when increasing N_2 initial pressure, which can be explained by the growing molecules adsorbed on the silica surface at higher pressure. It is demonstrated that under the same N_2 initial pressure, the average adsorption strength of oil molecules to silica shale channel increases with decreasing channel pore size. This is caused by larger surface-to-volume ratio in smaller pore channel, in which the proportion of oil molecules adsorbed on to the silica surface is larger. As noted, the cut-off distance in the simulation is 9.5 Å, which means almost all the oil molecules in the 3 nm silica shale channel are endowed an attractive interaction from the silica surface except for the small amount (1/9) in the middle of the channel. But this effect gradually decreased as the increasing of the pore size, leading to the decreased average adsorption strength of oil molecules to silica surface.

N_2 number effect

The effect of N_2 amount, temperature and shale component on the N_2 driving efficiency of the oil transportation inside 3 nm silica shale channel is investigated with N_2 initial pressure of 30 Mpa. The N_2 flooding with same N_2 pressure but different N_2 amount (the number of N_2 is 150, 300, 450, 600 and 750) as the driving force can trigger off the translocation of oil molecules inside 3 nm silica shale channel, as shown in Fig. 7, which demonstrate the snapshots of the final configuration of these models after a 2.5 ns simulation. It can be found that 150 N_2 molecules make the oil molecules center to move 5.236 Å in Fig. 7(a), while 300 N_2 molecules render them to move 26.827 Å in Fig. 7(b) and 750 N_2 molecules drive them to transport 30.175 Å shown in Fig. 7(e). Therefore, we suggest that the continuous driving force generated by 750 N_2 molecules is larger than that by 150 and 300 N_2 molecules and the increase of N_2 molecules is beneficial to the reduction of the extracting time of oil molecules from silica shale channels. As shown in Fig. 7, the displacement distance of oil molecules displays roughly linear on the number of N_2 molecules, resulting the increasing translocation rate of oil molecules. When the N_2 molecule number is 750, velocity of oil movement can reach up to 12.07 Å/ns, almost six times faster than that in the case of 150 N_2 molecules, 2.094 Å/ns. Another point should be noticed is that the displacement distance of oil molecules are quite similar when the number of N_2 molecules is larger than 300.

Temperature effect

Some previous investigations indicated that shale oil are relatively easy to be recovered from nano-scale pore-throats in subsurface shale under high temperature theoretically.[6,43] Previously, we have studied the effect of temperature on the adhesion energy between the polymers and SWNTs.[44,45] Using the same method, we have carried out additional MD simulations at different temperatures on the system of 3 nm silica shale channel with N_2 initial pressure of 30 Mpa to study the temperature effect. The temperatures vary from 348 K to 498 K
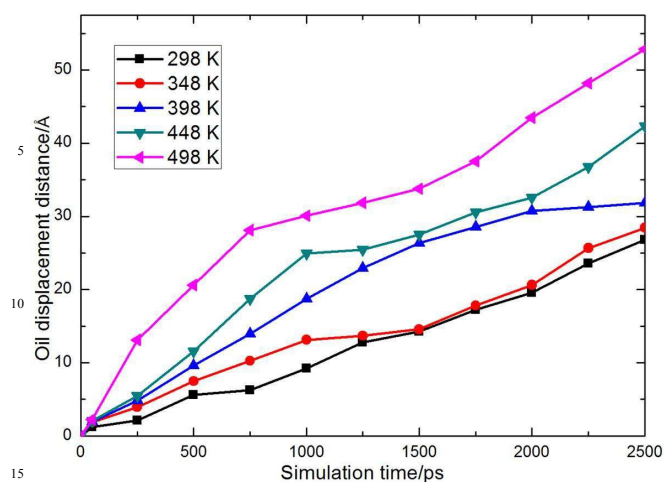

Fig. 7 Final configurations of N_2 driving oil transport in 3 nm silica shale channel with N_2 number of (a) 150, (b) 300, (c) 450, (d) 600 and (e) 750.

Fig. 8 Oil displacement inside 3 nm silica shale channel after N2 driving with 30 Mpa N_2 initial pressure as a function of simulation time under different temperatures.

in steps of 50 K. The oil displacement distance is compared with the results obtained at 298 K in Figure 8 as a function of simulation time.

As shown in Fig. 8, a higher temperature is beneficial to stimulate the oil molecules translocation in the same channel under same N_2 pressure. The oil droplet was firstly observed a displacement distance of 2 Å at ~250 ps during the driving simulation for the temperature of 298 K, while this displacement distance was generated at 25 ps with the temperature of 498 K, almost 10 times faster than that of 298 K. From the 250 ps to 2500 ps, the higher the temperature is, the more the oil center displacement distance is when reaching the same simulation time. After 2.5 ns simulation, the oil center displacement is 26.827 Å, 28.437 Å, 31.827 Å, 42.317 Å and 52.827 Å for the temperature of 298 K, 348 K, 398 K, 448 K and 498 K, respectively. Higher temperature cause higher oil displacement distance which is conducive to enhance the yields and velocity of oil recovery. It is possibly attributed to the higher kinetic energy of the fluid, which cause the instability of oil molecules thermodynamically,[46] as we can observe from the molecular dynamic trajectories, the explanation is in accordance with the water molecules transport in carbon nanotubes at higher temperature.[27]

Shale component effect

Seen from the previous calculations, the sorption characteristics of oil to silica shale channel is greatly determined by the adsorption interaction energy between oil molecules and shale substrates, which makes a difference on the final oil driving efficiency and yield. In general, the shale components have either high Si ratios, such as silica, or enriched with carbonate, such as calcite and dolomite. Therefore, we further simulate the N_2 driving oil transport process in calcite and dolomite shale channels to investigate the effect of shale component on the transportation properties of oil molecules inside shale channels and the final configurations of oil molecules inside the three different shale channels after a 2.5 ns simulation are shown in Fig. 9.

It can be found that a distinct oil transport happened for silica channel and calcite channel, indicating that the N_2 flooding is capable to impel oil molecules moving in these two channels. For silica channel, the oil center displacement distance is appropriate 26.827 Å, while it is much shorter in calcite channel and reaches to about 11.3 Å at the end of the simulation. On the country, for oil droplet in dolomite channel, the oil center almost keeps its position during the whole simulation, except for some spreading of oil molecules to the dolomite surface.

The different oil transportation properties should be ascribed to the different interaction between oil molecules and shale channels. Here, the interactions are calculated as Equation (1). The dolomite component showed the strongest interaction energy of 359.1 Kcal/mol and it is followed by calcite component of 275.12 Kcal/mol. However, the silica substrate holds the slightest interaction energy of only 43.98 Kcal/mol. It is obvious that the higher the interaction energy is, the harder the translocation process is, the stronger the oil adsorption strength to shale surface is, and so the critical pressure of gas flooding to transport oil molecules inside shale channel is larger. In other words, the start-up pressure of oil transportation inside the dolomite shale channel is the largest, when the sizes of the shale channels are the same.
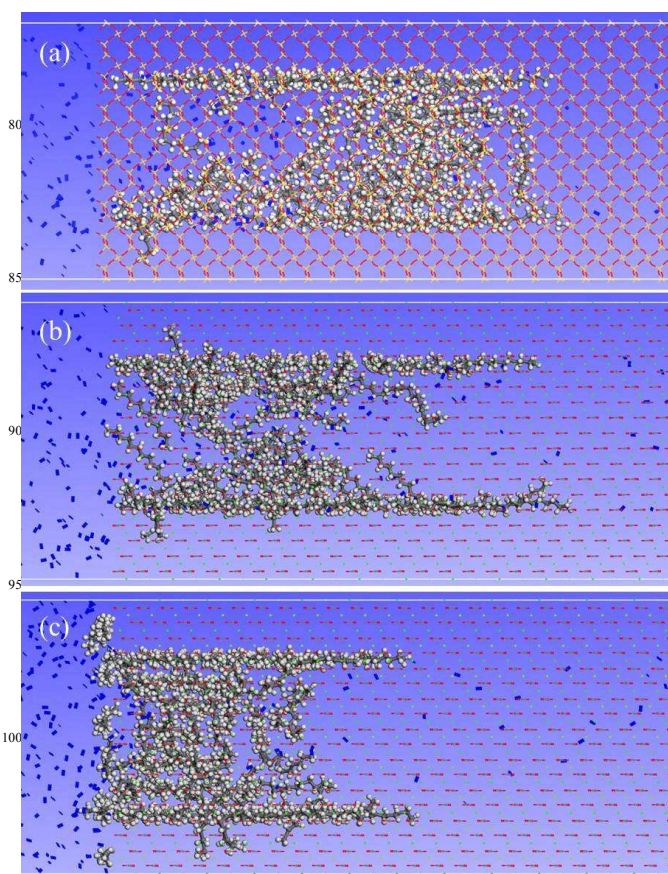

Fig. 9 Final configurations of oil molecules inside (a) silica, (b) calcite and (c) dolomite channels after N_2 driving.

Conclusion

In summary, the mechanism of oil molecules transportation in nano-sized shale channel was firstly explored using MD simulation. It is demonstrated that N_2 flooding can successfully drive dodecane molecules to transport in silica and calcite shale channel when the gas pressure reaches a critical value, called

start-up pressure. Further simulations identified that channel size, N_2 amount, temperature and shale component all have influences on the start-up pressure of driving oil molecules translocation and oil translocation efficiency. This can be explained by the competition between the adsorbed strength of the shale surface and the driving force from the N_2 flooding. Oil translocation in bigger pore size channel displays an apparent increase in oil displacement distance and decrease in oil displacement loss. Moreover, the adding of N_2 molecules number and the increasing of temperature are also favourable to the translocation of the oil droplet and the driving rate is also enhanced. The oil molecules in dolomite channel are hard to translocate under the present driving pressure. Our findings will provide insights to predict oil or viscous fluid transport in nano-sized channels, and develop reservoir simulators for production optimization.

Supporting information

Electronic Supplementary Information (ESI) available: It contains figure and video, Figure s1: Oil concentration profile in final configuration of N_2 driving oil transport in shale channel with N_2 initial pressure of 0 Mpa, 10 Mpa, 20 Mpa and 40 Mpa. Video S1: MD simulation showing 2.5 ns simulation of 30 Mpa N_2 flooding driving oil molecules in a 3 nm silica channel.

Acknowledgements

References

1. Hughes, J. D., *Nature*, 2013, **494** (7437), 307-308.

2. Wang, S.; Jiang, X.; Han, X.; Tong, J., *Energy*, 2012, **42** (1), 224-232.

3. Javadpour, F.; Fisher, D.; Unsworth, M., Journal of *J. Can. Pet. Technol.*, 2007, **46** (10), 55-61.

4. Mohaghegh, S. D., *J. Nat. Gas Sci. Eng.*, 2013, **12**, 22-33.

5. Jiang, X.; Han, X.; Cui, Z., *Energy*, 2007, **32** (5), 772-777.

6. Zou, C.; Yang, Z.; Cui, J.; Zhu, R.; Hou, L.; Tao, S.; Yuan, X.; Wu, S.; Lin, S.; Wang, L., *Adv. Pet. Explor. Dev.*, 2013, **40** (1), 15-27.

7. Ross, D. J.; Marc Bustin, R., *Mar. Pet. Geol.*, 2009, **26** (6), 916-927.

8. Zhong, J.; Wang, X.; Du, J.; Wang, L.; Yan, Y.; Zhang, J., *J. Phys. Chem. C*, 2013, **117** (24), 12510-12519.

9. Hu, H.; Li, X.; Fang, Z.; Wei, N.; Li, Q., *Energy*, 2010, **35** (7), 2939-2944.

10. Liu, Q.; Yuan, S.; Yan, H.; Zhao, X., *J. Phys. Chem. B*, 2012, **116** (9), 2867-2875.

11. Du, H.; Miller, J. D., *Langmuir*, 2007, **23** (23), 11587-11596.

12. Hu, X.; Li, Y.; Sun, H.; Song, X.; Li, Q.; Cao, X.; Li, Z., *J. Phys. Chem. B*, 2010, **114** (27), 8910-8916.

13. Tummala, N. R.; Shi, L.; Striolo, A., *J. Colloid Interface Sci.*, 2011, **362** (1), 135-143.

14. Zhong, J.; Wang, P.; Zhang, Y.; Yan, Y.; Hu, S.; Zhang, J., *Energy*, 2013, **59**, 295-300.

15. Salehi, M.; Johnson, S. J.; Liang, J.-T., *Langmuir*, 2008, **24** (24), 14099-14107.

16. van Duin, A. C.; Larter, S. R., *Org. Geochem.*, 2001, **32** (1), 143-150.

17. Vinegar, H. J.; De Rouffignac, E. P.; Maher, K. A.; Schoeling, L. G.; Wellington, S. L., *Google Patents*, 2010.

18. De Rouffignac, E. P.; Berchenko, I. E.; Fowler, T. D.; Karanikas, J. M.; Maher, K. A.; Ryan, R. C.; Shahin Jr, G. T.; Vinegar, H. J.; Wellington, S. L.; Zhang, E., *Google Patent*, 2005.

19. Huang, C.; Nandakumar, K.; Choi, P. Y.; Kostiuk, L. W., *J. Chem. Phys.*, 2006, **124** (23), 234701.

20. Thomas, J. A.; McGaughey, A. J.; Kuter-Arnebeck, O., *Int. J. Therm. Sci.*, 2010, **49** (2), 281-289.

21. Thomas, J. A.; McGaughey, A. J., *Phys. Rev. Lett.*, 2009, **102** (18), 184502.

22. Carvalho, E. J.; dos Santos, M. C., *Acs Nano*, 2010, **4** (2), 765-770.

23. Li, Y.; Xu, J.; Li, D., *Microfluid. Nanofluid.*, 2010, **9** (6), 1011-1031.

24. Joseph, S.; Aluru, N., *Nano lett.*, 2008, **8** (2), 452-458.

25. Thomas, J. A.; McGaughey, A. J., *Nano lett.*, 2008, **8** (9), 2788-2793.

26. Walther, J. H.; Ritos, K.; Cruz-Chu, E. R.; Megaridis, C. M.; Koumoutsakos, P., *Nano lett.*, 2013, **13** (5), 1910-1914.

27. Kotsalis, E.; Walther, J. H.; Koumoutsakos, P., *Int. J. Multiphase Flow*, 2004, **30** (7), 995-1010.

28. Yu, H.; Li, H.; Zhang, J.; Liu, X.; Liew, K. M., *Carbon*, 2010, **48** (2), 417-423.

29. Xue, Q.; Jing, N.; Chu, L.; Ling, C.; Zhang, H., *RSC Adv.*, 2012, **2** (17), 6913-6920.

30. Ghadimi, A.; Saidur, R.; Metselaar, H., *Int. J. Heat Mass Transfer*, 2011, **54** (17), 4051-4068.

31. Saidur, R.; Leong, K.; Mohammad, H., *Renewable Sustainable Energy Rev.*, 2011, **15** (3), 1646-1668.

32. Mahian, O.; Kianifar, A.; Kalogirou, S. A.; Pop, I.; Wongwises, S., *Int. J. Heat Mass Transfer*, 2013, **57** (2), 582-594.

33. Yu, W.; Xie, H., *J. Nanomater.*, 2012, **2012**, 1.

34. Liang, Z.; Tsai, H.-L., *Microfluid. Nanofluid.*, 2012, **13** (2), 289-298.

35. Sun, H., *J. Phys. Chem. B*, 1998, **102** (38), 7338-7364.

36. Sun, H.; Ren, P.; Fried, J., *Comput. Theor. Polym. Sci.*, 1998, **8** (1), 229-246.

37. Rigby, D.; Sun, H.; Eichinger, B., *Polymer International*, 1997, **44** (3), 311-330.

38. Liu, Z.; Xue, Q.; Xing, W.; Du, Y.; Han, Z., *Nanoscale*, 2013, **5** (22), 11132-11138.

39. Tao, Y.; Xue, Q.; Liu, Z.; Shan, M.; Ling, C.; Wu, T.; Li, X., *ACS Appl. Mater. Interfaces*, 2014, **6**(11), 8048-8058.

40. Liu, Z.; Xue, Q.; Ling, C.; Yan, Z.; Zheng, J., *Comput. Mater. Sci.*, 2013, **68**, 121-126.

41. Yan, K.; Xue, Q.; Xia, D.; Chen, H.; Xie, J.; Dong, M., *Acs Nano*, 2009, **3** (8), 2235-2240.

42. Tao Y.; Xue, Q.; et al. *Sci. of Adv. Mater.*, 2014, 2015, **7**(2), 239-248(10).

43. Na, J. G.; Im, C. H.; Chung, S. H.; Lee, K. B., *Fuel*, 2012, **95**, 131-135.

44. Zheng, Q.; Xue, Q.; Yan, K.; Hao, L.; Li, Q.; Gao, X., *J. Phys. Chem. C*, 2007, **111** (12), 4628-4635.

45.Chen, H.; Xue, Q.; Zheng, Q.; Xie, J.; Yan, K., *J. Phys. Chem. C*, 2008, **112** (42), 16514-16520.
46.Zhan, J.-H.; Wu, R.; Liu, X.; Gao, S.; Xu, G., *Fuel* , 2014, **134**, 283-292.
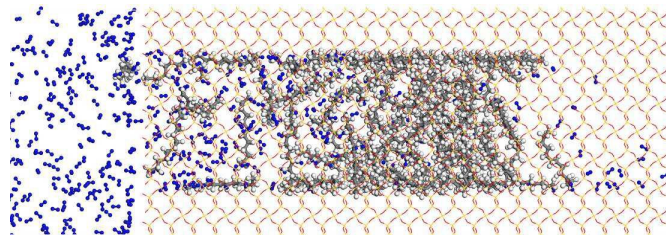
5

Graphic Abstract

Table of contents text: Driving oil molecules along nano-sized shale channels using nitrogen molecules: MD simulation